



J. Serb. Chem. Soc. 85 (10) S468–S472 (2020)

SUPPLEMENTARY MATERIAL TO
Systematic profiling of ATP response to acquired drug-resistant EGFR family kinase mutations

DINGWA ZHANG^{1*}, DEYONG HE¹, XIAOLIANG PAN² and LIJUN LIU^{1**}

¹School of Chemistry and Chemical Engineering, Jinggangshan University, Ji'an 343009, China and ²School of Mechanical and Electrical Engineering, Jinggangshan University, Ji'an 343009, China

J. Serb. Chem. Soc. 85 (10) (2020) 1265–1278

Structural modeling of ATP complex structures with wild-type and mutant ErbB kinase domains

The complex structure of the active EGFR kinase domain with an ATP–peptide conjugate was retrieved from the PDB database¹ with id 2GS6. The structure is a reaction intermediate of kinase-catalyzed transfer of the ATP phosphate group to the peptide substrate. Therefore, it would represent the real active binding mode of ATP to the active site of EGFR. As could be seen in Fig. S-1, the conjugate consists of an ATP molecule and a peptide substrate, in which the ATP phosphate moiety was just covalently bonded to the hydroxyl group of peptide tyrosine residue. The peptide can be readily removed from the structure leaving an ATP analog using a manual modification approach, which was manually modified to ATP molecule and then subjected to QM/MM energy minimization, finally resulting in the modeled complex structure of the EGFR kinase domain with ATP, in which, evidently, the ATP molecule adopts a “correct” binding mode to interact with the kinase active site, in which the purine ring of ATP tightly packs against the active site, while exposing its triphosphate moiety to the solvent.

The modeled complex structure of the EGFR kinase domain with ATP was used as a structural template to further model the complex structures of other three ErbB kinase domains as well as their drug-resistant mutants with ATP. In the procedure, the *apo* crystal structure of ErbB2, ErbB3 and ErbB4 kinase domains were retrieved from the PDB database with ids 3PP0, 3LMG and 3BCE, respectively. A ligand grafting method was employed to model the complex structures of ErbB2, ErbB3 and ErbB4 kinase domains with ATP, *i.e.*, the *apo*

*,** Corresponding authors. E-mail: (*)lij_liu@163.com; (**)dwzhang@163.com

structures of Her2, Her3 and Her4 kinase domains were superposed onto the template of EGFR kinase domain–ATP complex, and then the EGFR kinase domain was manually removed from the superposed system to obtain the modeled complexes of ErbB2, ErbB3 and ErbB4 kinase domains with ATP. Next, the wild-type EGFR, ErbB2, ErbB3 and ErbB4 kinase domains in these complex structures were automatically mutated to their drug-resistant mutants in the PyMol program,² which were then subjected to QM/MM energy minimization. Consequently, a total 41 ATP complex structures with the 4 wild-type ErbB kinase domains and their 37 drug-resistant mutants were systematically obtained.

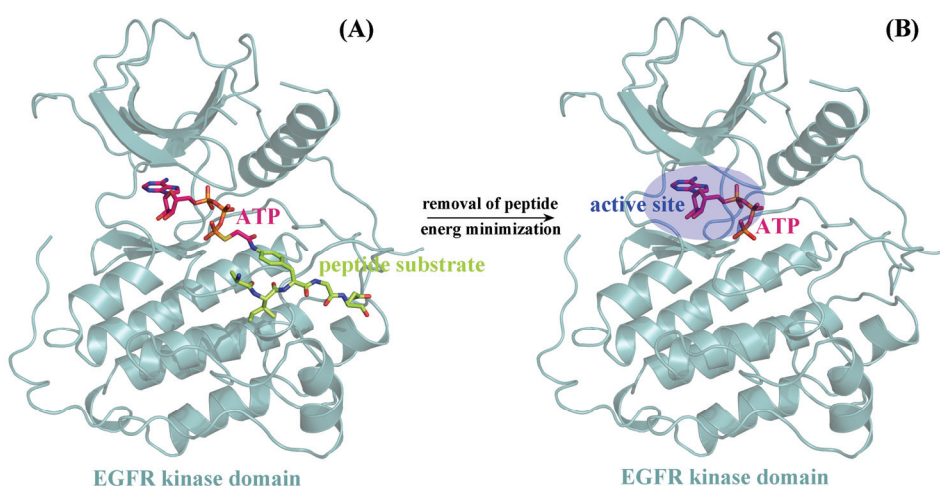


Fig. S-1. A) Crystal structure of EGFR kinase domain in a complex with an ATP-peptide conjugate (PDB: 2GS6). B) The peptide substrate was manually removed from the structure to generate the complex of EGFR kinase domain with ATP, which was then minimized by QM/MM.

IN VITRO KINASE ASSAY

A standard protocol modified from previous reports^{3,4} was used to perform the kinase assays. The kinase proteins were diluted in a final volume of 50 μ L assay buffer containing 50 mM Tris-HCl (pH 7.8), 20 mM $MgCl_2$, 1 mM $MnCl_2$ and 1 mM DTT containing 10 μ M substrate peptides, 5 μ M ATP and 1 μ Ci [γ -³²P]ATP. The reaction was incubated with increasing concentrations of inhibitor compound at room temperature for 30 min and then stopped by the addition of SDS-sample loading buffer. The samples were loaded in an SDS-PAGE gel and then exposed to X-ray beam for radioactive detection. The phosphorylated substrates were plotted against the concentration of inhibitor to determine the IC_{50} value for kinase inhibition. The recombinant proteins of ErbB1 and ErbB2 kinase domains were obtained commercially. The inhibitor compounds Gefitinib and Lapatinib were suspended in DMSO and stored until use in small aliquots at -20 $^{\circ}C$.

Surface plasmon resonance analysis

All surface plasmon resonance (SPR) experiments were performed on a Biacore T100 with active temperature control at 25 °C following the manufacturer's protocols and previous reports.^{5,6} ErbB2 kinase domain proteins were immobilized onto activated a CM5 sensor chip by standard amine coupling. All interaction experiments were performed in a buffer containing 50 mM Tris-HCl, 100 mM NaCl, 15 mM MgCl₂ and 0.05 % Tween-20. The ATP was injected at different concentrations varying between 1 and 500 nM at a flow rate of 50 μL min⁻¹. Changes in surface concentration are proportional to changes in the refractive index on the surface, resulting in changes in the SPR signal. For all samples, blank injection with buffer alone was subtracted from the resulting reaction surface data. The data were analyzed using Biacore evaluation software and fitted using GraphPad Prism software.

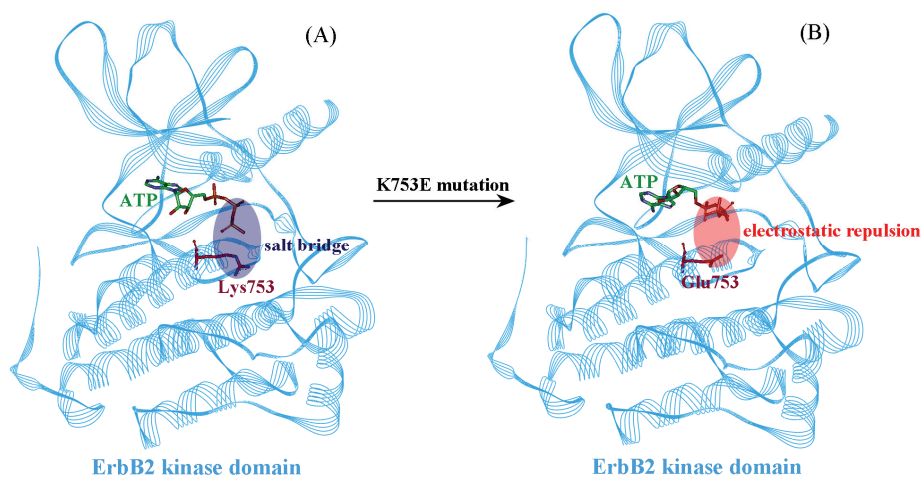


Fig. S-2. The binding mode change of drug-resistant ErbB2 mutation K753E on ATP binding mode to the kinase.

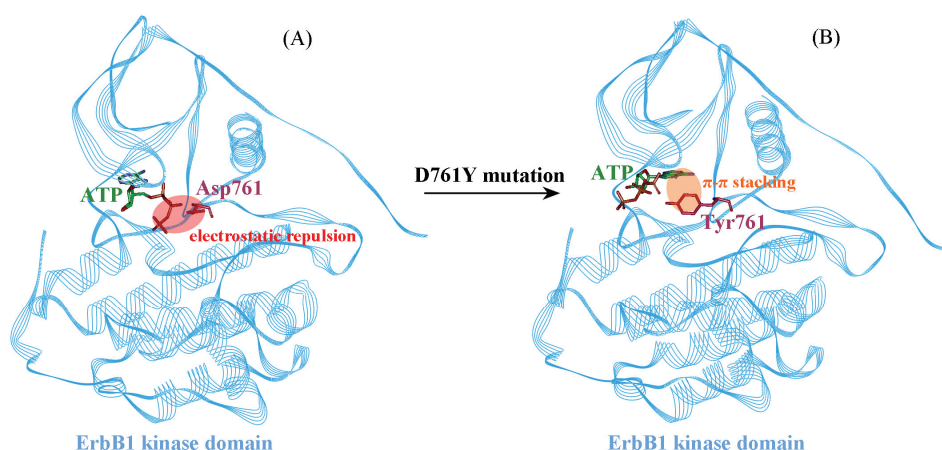


Fig. S-3. The binding mode change of drug-resistant ErbB1 mutation D761Y on ATP binding mode to the kinase.

TABLE S-I. The 37 acquired drug-resistant ErbB kinase mutations involved in human cancers

ErbB kinase	Mutation ^a	Resistant TKI	Human cancer
ErbB1/EGFR	L718Q	CO-1686, WZ4002	NSCLC
ErbB1/EGFR	L747S	Erlotinib, Gefitinib	NSCLC
ErbB1/EGFR	L844V	WZ4002, CO-1686	NSCLC
ErbB1/EGFR	D761Y	Gefitinib	Brain tumor
ErbB1/EGFR	V769M	Erlotinib, Gefitinib	NSCLC
ErbB1/EGFR	T790M*	Erlotinib, Gefitinib	NSCLC
ErbB1/EGFR	L792F	Osimertinib	NSCLC
ErbB1/EGFR	L792H	Osimertinib	NSCLC
ErbB1/EGFR	G796S	Osimertinib	NSCLC
ErbB1/EGFR	G796R	Osimertinib	NSCLC
ErbB1/EGFR	C797S	Osimertinib	NSCLC
ErbB1/EGFR	T854A	Erlotinib, Gefitinib	NSCLC
ErbB1/EGFR	L858R	Osimertinib	NSCLC
ErbB1/EGFR	A871E	Erlotinib, Gefitinib	NSCLC
ErbB2	L726I	Gefitinib	Breast cancer
ErbB2	L726F	Lapatinib	Breast cancer
ErbB2	K753I	Lapatinib	Breast cancer
ErbB2	K753E	Lapatinib	Breast cancer
ErbB2	L755S	Lapatinib	Breast cancer
ErbB2	L755P	Lapatinib	Breast cancer
ErbB2	P780L	Lapatinib	Breast cancer
ErbB2	S783P	Lapatinib	Breast cancer
ErbB2	L785F	Lapatinib	Breast cancer
ErbB2	T798I*	Neratinib	Breast cancer
ErbB2	T798M*	Lapatinib	Breast cancer
ErbB2	V842I	Lapatinib	Breast cancer
ErbB3	T768I*	Bosutinib	Breast cancer
ErbB3	Q809R	Neratinib	Breast cancer
ErbB3	S846I	Neratinib	Breast cancer
ErbB3	V855A	Pertuzumab, Afatinib	NSCLC
ErbB3	E928G	Neratinib	Breast cancer
ErbB4	R711C	Lapatinib	Breast cancer
ErbB4	L798R	Lapatinib	Breast cancer
ErbB4	R847C	Lapatinib	Breast cancer
ErbB4	R847H	Lapatinib	Breast cancer
ErbB4	R992C	Lapatinib	Breast cancer
ErbB4	R992S	Lapatinib	Breast cancer

^aThe asterisk '*' indicates gatekeeper mutation.

REFERENCES

1. H. M. Berman, J. Westbrook, Z. Feng, G. Gilliland, T. N. Bhat, H. Weissig, I. N. Shindyalov, P. E. Bourne, *Nucleic Acids Res.* **28** (2000) 235
(<https://doi.org/10.1093/nar/28.1.235>)
2. S. Yuan, H. C. S. Chan, Z. Hu, *WIREs Comput. Mol. Sci.* **7** (2017) e1298
(<https://doi.org/10.1002/wcms.1298>)

3. X. Ai, Y. Sun, H. Wang, S. Lu, *Amino Acids* **46** (2014) 1635
(<https://doi.org/10.1007/s00726-014-1716-0>)
4. Z. Wang, M. Jiang, N. Feng, C. Li, *Biochimie* **52** (2018) 188
(<https://doi.org/10.1016/j.bioci.2018.07.005>)
5. K. T. Kuo, W. C. Lin, K. C. Chang, J. Y. Huang, K. C. Yen, I. C. Young, Y. J. Sun, F. H. Lin, *PLoS ONE* **10** (2015) e0116610 (<https://doi.org/10.1371/journal.pone.0116610>)
6. Y. Zhao, Y. Jiao, F. Sun, X. Liu, *Med. Chem. Res.* **27** (2018) 2160
(<https://doi.org/10.1007/s00044-018-2224-7>).